DOI 10.1007/978-1-4939-2038-9_24
Reprinted from *Solar Physics* Journal, DOI 10.1007/s11207-014-0515-9

On the Origin of Pulsations of Sub-THz Emission from Solar Flares

V.V. Zaitsev · A.V. Stepanov · P. Kaufmann

Received: 26 November 2013 / Accepted: 4 March 2014 / Published online: 18 March 2014
© Springer Science+Business Media Dordrecht 2014

Abstract We propose a model to explain fast pulsations in sub-THz emission from solar flares. The model is based on the approach of a flaring loop as an equivalent electric circuit and explains the pulse-repetition rate, the high-quality factor, $Q \geq 10^3$, low modulation depth, pulse synchronism at different frequencies, and the dependence of the pulse-repetition rate on the emission flux, observed by Kaufmann *et al.* (*Astrophys. J.* **697**, 420, 2009). We solved the nonlinear equation for electric current oscillations using a Van der Pol method and found the steady-state value for the amplitude of the current oscillations. Using the pulse rate variation during the flare on 4 November 2003, we found a decrease of the electric current from 1.7×10^{12} A in the flare maximum to 4×10^{10} A just after the burst. Our model is consistent with the plasma mechanism of sub-THz emission suggested recently by Zaitsev, Stepanov, and Melnikov (*Astron. Lett.* **39**, 650, 2013).

Keywords Solar flares · Sub-terahertz emission · Pulsations · Electric circuit

1. Introduction

Observations of sub-THz emission from solar flares at 212 and 405 GHz (Kaufmann *et al.*, 2004, 2009) have posed new questions for solar physicists. These observations revealed a W-shaped spectrum of the emission instead of the well-known U-shaped one: the emission

V.V. Zaitsev
Institute of Applied Physics, Ulianova str. 46, Nizhny Novgorod 603950, Russia
e-mail: za130@appl.sci-nnov.ru

A.V. Stepanov (✉)
Pulkovo Observatory, Pulkovo chaussee 65, Saint Petersburg 196140, Russia
e-mail: stepanov@gao.spb.ru

P. Kaufmann
Centro de Rádio-Astronomia e Astrofísica Mackenzie, Escola de Engenharia, Uniersidade Presbiteriana Mackenzie, Rua Consolação 896, 01302-907 São Paulo, SP, Brazil
e-mail: kaufmann@craam.mackenzie.br

flux grows from frequencies > 30 GHz and extends towards the THz domain. This suggests some unknown mechanism of the solar radio emission.

Various attempts to explain the origin of this mysterious spectral component were made, based on free–free emission, gyrosynchrotron radiation, and synchrotron emission of electrons with the energy exceeding 10 MeV in a strong (≥ 1000 G) magnetic field. Fleishman and Kontar (2010) suggested Cherenkov emission from chromospheric layers. Unlike those in the corona, atoms and molecules in the partially ionized chromosphere contribute positively to the dielectric permittivity, $\varepsilon(\omega)$, which may exceed unity; therefore, the particle velocity, $V > c/\sqrt{\varepsilon(\omega)}$, and Cherenkov radiation is indeed possible. However, the acceleration mechanism of electrons with energies higher than 10 MeV is still unknown, and, in the case of Cherenkov radiation, a more detailed calculation of $\varepsilon(\omega)$ and radiation flux is needed. An alternative interpretation suggests a plasma radiation mechanism that is quite efficient under the conditions of the solar and stellar coronae (Zheleznyakov, 1997; Zaitsev and Stepanov, 1983; Stepanov *et al.*, 1999, 2001). A coherent plasma radiation mechanism implies the excitation of plasma waves driven by a beam or loss-cone instability and subsequently, the conversion of plasma waves into electromagnetic radiation at the electron plasma frequency and at its second harmonic due to Rayleigh and Raman scattering. One attempt to simulate the THz spectral component in terms of plasma radiation was undertaken by Sakai *et al.* (2006), who simulated the generation of Langmuir waves by high-energy electron beams. A recent review of sub-THz emission mechanisms has been published in Krucker *et al.* (2013).

Plasma mechanism of sub-THz emission proposed recently by Zaitsev, Stepanov, and Melnikov (2013) suggests that the emission source is localized at the chromospheric footpoints of coronal magnetic loops, where the electron density is $n \geq 10^{14}$ cm^{-3}. This requires the chomosphere to be heated to coronal temperatures at heights ≈ 500 km, which provides the high degree of ionization needed for Langmuir frequencies, 200 – 400 GHz. Zaitsev, Stepanov, and Melnikov (2013) have shown that the electron acceleration and plasma heating in the sub-THz source can occur when the ballooning mode of the flute instability develops at the chromospheric footpoints of a flare loop. The flute instability deforms the magnetic field at the loop footpoints. Thus, the electric current flowing in the loop changes and an inductive electric field appears. This field causes the acceleration of electrons that do not escape from the chromosphere, providing the excitation of plasma waves and the *in situ* heating of the chromospheric plasma. The heated chromospheric plasma evaporates from the loop footpoints, heats the overlying layers of the solar atmosphere and thereby reduces free–free absorption of the generated sub-THz emission. It is important to note that the observations with the *New Solar Telescope* at Big Bear Solar Observatory (Ji, Cao, and Goode, 2012) give us distinct indications on the heating of chromospheric footpoints of thin coronal loops to coronal temperatures as well as upward injection of hot plasma that excite the thin loops from the photosphere to the base of the corona.

The best observed sub-THz flaring events were accompanied by fast (second and subsecond) pulsations superimposed on the main bursts. The most important peculiarities of such pulsations are the high quality-factor, Q, pulse synchronism at different frequencies, and a puzzling linear relationship between pulse-repetition rate and mean emission fluxes. This proportionality was previously indicated qualitatively at 10 – 90 GHz (Kaufmann *et al.*, 1980). It might be interpreted as a response to discrete and successive energetic injections, quantized in energy (Kaufmann *et al.*, 1980, 2009). Other interpretations suggested the emission modulation by magnetic-field variations driven by magneto-hydrodynamic (MHD) oscillations of a coronal loop (Qin *et al.*, 1996) or due to wave–particle plasma instabilities with a saturation time inversely proportional to the radiation time (Huang, Qin, and Yao, 1996).

At the same time, pulsations with a high Q-factor in solar and stellar flares were explained successfully by the model of a current-carrying loop as an equivalent electric (RLC) circuit (Zaitsev *et al.*, 1998, 2001; Stepanov, Zaitsev, and Nakariakov, 2012; Stepanov and Zaitsev, 2013). Here, we analyze rapid pulsations of sub-THz emission considering a flaring loop as an equivalent electric circuit. This idea was first formulated by Alfvén and Carlqvist (1967) for the circuit model of a flare. Later, the electric-circuit approach was successfully developed by numerous authors (*i.e.* Sen and White, 1972; Ionson, 1982; Kan, Akasofu, and Lee, 1983; Zaitsev and Stepanov, 1992; Cargill, Ghen, and Garren, 1994; Zaitsev *et al.*, 1998; Tan *et al.*, 2007; Khodachenko *et al.*, 2009) and used as an effective diagnostic tool of flaring plasma. In this article, we try to explain the observed peculiarities of pulsations of sub-THz emission in terms of an RLC-circuit and present additional arguments in favor of the plasma mechanism of this emission.

2. Pulsation Characteristics

Time profiles of sub-THz emission from solar flares reveal rapid pulsations with some peculiarities (Raulin *et al.*, 2003; Makhmutov, Raulin, and de Castro, 2003; Kaufmann *et al.*, 2004, 2009). Kaufmann *et al.* (2009) presented the most comprehensive study of pulsation characteristics at 212 and 405 GHz using the data for the events on 2 and 4 November 2003, and 6 December 2006, obtained with the *Solar Submillimeter Telescope* (Kaufmann *et al.*, 2008). The superimposed pulsations displayed a repetition rate, $\nu_{\rm r}(t)$, from 0.2 $\rm s^{-1}$ to 8.5 $\rm s^{-1}$. A remarkable peculiarity was the similarity of the time profile of $\nu_{\rm r}(t)$ to that of the flux density $F(t)$ (see Figure 3 in Kaufmann *et al.*, 2009).

The radiation flux density, F, at 212 and 405 GHz depends on the repetition rate $\nu_{\rm r}$ linearly as a rule, with very large correlation coefficients. The scatter diagram for the event on 4 November 2003 (Figure 1a) yields $F = k\nu_{\rm r}$, where $k = 400$ sfu at 405 GHz and $k = 800$ to 1200 sfu at 212 GHz.

Because of the poor atmospheric transmission on 6 December 2006, the data for this event (Figure 1b) were substantially more scattered than those for the event on 4 November 2003 (Figure 1a). As a result, for the event on 6 December 2006, the linear correlation between the flux and repetition rate is less evident, and the dependence of $F(\nu_{\rm r})$ for 212 GHz may even be quadratic, $F \sim \nu_{\rm r}^2$.

In all events studied by Kaufmann *et al.* (2009), the typical modulation depth of the pulsations was about 5 – 8 %. Note that observations at 44 GHz show a modulation depth up to 80 % (Kaufmann *et al.*, 2009). This suggests that sub-mm emission might have a different physical origin. Important distinctions of the rapid pulsations in sub-THz are synchronism at different frequencies and their high Q-factor. For example in the decay pulsation phase of the 4 November 2003 flare (Figure 5 of Kaufmann *et al.*, 2004) the Q-factor is $Q = \pi D\nu_{\rm r} \approx 850$, where D is the exponentially decaying train duration. This estimation can be considered as a minimum value of Q because rapid pulsations were observed throughout the burst durations of about 10 min. Therefore, the sub-THz pulsation model should explain the pulse-repetition rate, the dependence, $F(\nu_{\rm r})$, the high quality of pulsations, $Q \geq 10^3$, the pulse synchronism, and low modulation depth compared with that observed at 44 GHz.

3. Review of Sub-THz Pulsation Models

The most popular models of pulsations in solar flares suggest that the pulsations originate from MHD oscillations of whole coronal magnetic loops. The oscillations modulate the

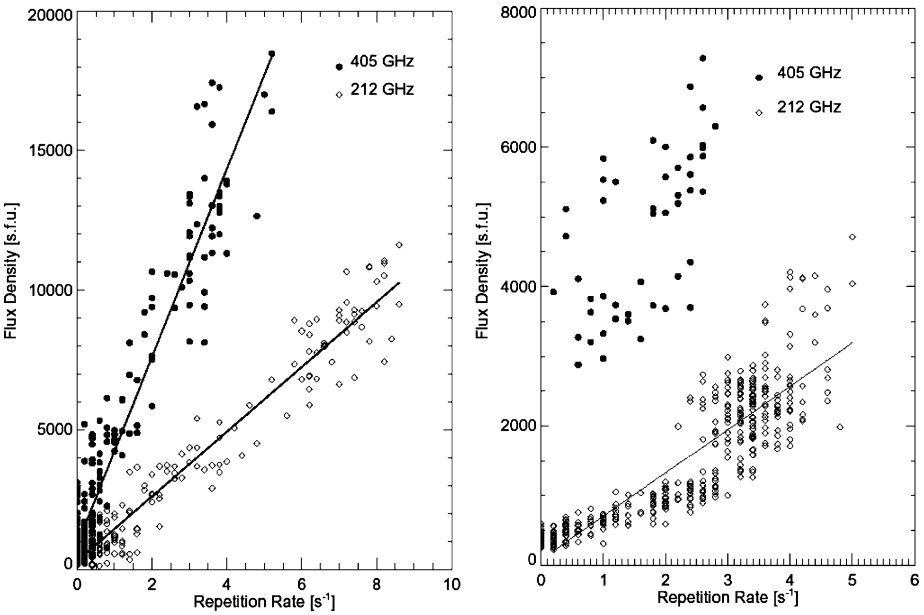

Figure 1 (a) The correlation between the flux and the pulse-repetition rate for the flare on 4 November 2003 at 212 GHz (open diamonds) and 405 GHz (filled circles). The best-fit linear correlation coefficients are 0.975 and 0.953 at 212 and 405 GHz, respectively. (b) The correlation between the flux density and pulse-repetition rate for the event on 6 December 2006 at 212 GHz (open diamonds) and 405 GHz (filled circles). The data are highly scattered because of poor atmospheric transmission. The best-fit linear correlation is 0.87 only at 212 GHz. The scatter at 405 GHz is too large to determine the correlation (Kaufmann *et al.*, 2009).

emission of accelerated electrons due to variations of the loop magnetic field and the number density of the accelerated particles. The period of the loop oscillations corresponds to the radial sausage mode:

$$P_{\rm saus} = \frac{2.6r}{\sqrt{c_{\rm A}^2 + c_{\rm s}^2}}, \tag{1}$$

where r is the minor radius of the loop, $c_{\rm A} = B/\sqrt{4\pi\rho}$ is the Alfvén velocity, $c_{\rm s} = \sqrt{10k_{\rm B}T/3m_{\rm i}}$ is the sound speed. For example, if the plasma average density in a coronal flaring loop is $n = 10^{12}$ cm^{-3} and the temperature $T = 10^6$ K with $\beta = 8\pi nk_{\rm B}T/B^2 < 1$, where $k_{\rm B}$ is the Boltzmann constant, which suggests a loop magnetic field $B \geq 100$ G, we have $\sqrt{c_{\rm A}^2 + c_{\rm s}^2} \approx 2.7 \times 10^7$ cm s^{-1}. Then the observed pulsation period $P \approx 0.1-5$ s can be explained if the minor radius of the coronal loop is sufficiently small, $r \approx (0.1-5) \times 10^7$ cm. Note that Equation (1) describes the period of sausage oscillations if the loop has a steep radial profile of the Alfvén speed. For smoother profiles the sausage-mode period becomes shorter (Nakariakov, Hornsey, and Melnikov, 2012). On the other hand, for "thick" loops the period of the global sausage mode can be several times longer than Equation (1) (Nakariakov, Melnikov, and Reznukova, 2003).

Based on Equation (1), Qin *et al.* (1996) have shown that the period of the sausage oscillations can decrease for higher plasma temperatures, but it requires $\beta = 3c_{\rm s}^2/5c_{\rm A}^2 > 1$. However, for $\beta > 1$, the flaring loop collapses very rapidly and high-quality pulsations be-

come impossible. The long train of pulsations is also unlikely to occur because of strong acoustic damping of loop-sausage oscillations.

In the slow magneto-acoustic mode, the oscillation period increases with the time because of the expansion of the heated region. In the kink mode, the period depends on the loop length, l, as $P \approx l/c_{\rm A} \geq 10$ s, and it cannot modulate a compact source at the loop footpoints with a period ≤ 1 s. Consequently, these two modes are inapplicable to the interpretation of the observations.

The linear correlation, $F(\nu_{\rm r})$, between the emission flux and pulse rate was also suggested by Huang, Qin, and Yao (1996) based on the inverse correlation between the saturation time of the plasma instability caused by the burst and the radiation flux. They assumed that as a result of this inverse correlation the sequence of spike bursts is formed with a spike-to-spike time interval that decreases with the increase in the radiation level. However, Huang, Qin, and Yao (1996) neither specified the type of the plasma instability that explains the linear dependence $F = k\nu_{\rm r}$ nor discussed reasons for the high Q-factor of the pulsations.

Zaitsev (1971) suggested a pulsation model of a "rain" type, using induced scattering of excited plasma waves on the ions of the thermal plasma. This nonlinear process of the transfer of plasma waves from the resonant (instability) domain to the nonresonant (damping) domain is described by Lotka–Volterra equations for the "predator–prey" problem:

$$\frac{{\rm d}w}{{\rm d}t} = \gamma w - \xi w w^*, \qquad \frac{{\rm d}w^*}{{\rm d}t} = \xi w w^* - \nu w^*. \tag{2}$$

Here, $w = W/nk_{\rm B}T$, $w^* = W^*/nk_{\rm B}T$, W and W^* are the energy densities of plasma waves in resonant and nonresonant regions of the phase velocities, respectively, γ is the instability growth rate, ξ is the coefficient of induced nonlinear transfer of plasma waves along the wave spectrum, ν is the wave decrement. Equation (2) allows periodic solutions that correspond to closed trajectories around a center-type point, $w_0 = \nu/\xi$ and $w_0^* = \gamma/\xi$. The pulse rate around this point is $\nu_{\rm nl} \approx (\gamma\nu)^{1/2}$. In the vicinity of the instability threshold ($\gamma \approx \nu = \nu_{\rm ei}$), for $T = 2 \times 10^6$ K and $n = (10^{10} - 5 \times 10^{14})$ cm^{-3} in the low corona and chromosphere (Zaitsev, Stepanov, and Melnikov, 2013) the electron–ion collision frequency is $\nu_{\rm ei} \approx 60\, n/T^{3/2} \approx (6 \times 10^2 - 10^7)$ s^{-1}. Because $\nu_{\rm nl} \approx \nu_{\rm ei} \gg \nu_{\rm r}$, the rain-type model does not explain the observed pulse rates in the sub-THz emission.

Some other models of pulsations are discussed, for example, quasi-periodical electron acceleration or injection (Fleishman, Bastian, and Gary, 2008), multiple-particle acceleration in the reconnection process (Kliem, Karlický, and Benz, 2000), and multiple-coalescence instabilities (Tajima, Brunel, and Sakai, 1982). However, these mechanisms cannot explain all peculiarities of rapid pulsations at 212 and 404 GHz described in Section 2. At the same time, in many cases the pulsations in solar and stellar flares were explained successfully by the model of a current-carrying loop as an equivalent electric (RLC) circuit (Zaitsev *et al.*, 1998; Stepanov, Zaitsev, and Nakariakov, 2012).

4. Oscillations of a Coronal Loop as an Equivalent Electric Circuit

The high Q-factor and phase synchronism of rapid pulsations at sub-THz are consistent with the electric current oscillations in a flaring loop as an equivalent electric circuit. Photospheric convective motions interacting with the magnetic field at the loop footpoints generate an electric current, which flows from one footpoint to the other through the coronal part of the loop and closes below the photosphere, where the conductivity becomes isotropic.

Therefore, a coronal magnetic loop with a subphotospheric current channel may be considered as a wire loop with electric current. In this case, we can write the equation for the equivalent electric circuit. For small deviations of the electric current, I, which flows along the loop axis, from the steady-state value, I_0, this equation can be represented as follows (*i.e.* Khodachenko *et al.*, 2009):

$$\frac{1}{c^2}L\frac{\mathrm{d}^2y}{\mathrm{d}t^2}+\left[R(I_0)-\frac{|V_\mathrm{r}|l_1}{c^2r_1}\right]\frac{\mathrm{d}y}{\mathrm{d}t}+\frac{1}{C(I_0)}y=0. \tag{3}$$

Here, $y=(I-I_0)/I_0$, L is the loop inductance, R is the loop resistance, C is the loop capacitance, V_r is the radial component of the velocity of the photosphere plasma in the footpoints of the loop. Approximating the flare loop as a wire with the length l and a minor radius $r \ll l$, we can use the well-known expression for the circular wire-loop inductance (Landau and Lifshitz, 1984):

$$L\approx 2l\left(\ln\frac{4l}{\pi r}-\frac{7}{4}\right). \tag{4}$$

The effective capacity, $C(I_0)$, depends on the electric current in the loop:

$$\frac{1}{C(I_0)}\approx\frac{I_0^2l}{c^4\rho\pi r_2^4}\left(1+b^{-2}\right). \tag{5}$$

The parameter b is determined by the magnetic-field components and the gas pressure at the loop axis and outside the loop:

$$b=\frac{B_{\varphi0}(r)}{B_{z0}(r)-B_{z0}(0)}\approx 6\frac{B_{\varphi0}(r)B_{z0}(0)}{8\pi[p(\infty)-p(0)]}. \tag{6}$$

Here, ρ is the loop plasma density, r_2 is the loop radius at the coronal part of the loop, $B_{\varphi0}$, B_{z0} are the azimuthal and axial components of the loop magnetic field. The effective loop resistance is determined as in Khodachenko *et al.* (2009),

$$R(I_0)\approx\frac{F_1^2I_0^2l_1}{(2-F_1)c^4n_1m_\mathrm{i}\nu'_\mathrm{ia}\pi r_1^4}\left(1+b^{-2}\right), \tag{7}$$

where l_1, r_1, n_1 are the height scale of the photospheric electromotive force, (emf), loop radius, electron number density, respectively, $F_1=\rho_\mathrm{a}/\rho$ is the relative density of neutrals in the chromosphere, and ν'_ia is the effective frequency of ion–atom collisions. The second term in Equation (3) is related to the emf of the equivalent electric circuit. The electromotive force appears due to the interaction of the velocity V_r with the azimuthal component of magnetic field, $B_\phi\sim I$. In Equation (3) for oscillations of the electric current in a loop, the emf appears as a negative resistance $R_{(-)}=-|V_\mathrm{r}|l_1/c^2r_1$.

A horizontal plasma flow into the loop appears due to either photospheric convection, when the loop footpoints are located at the nodes of several granulation cells, or the ballooning mode of the flute instability, as we suggested analyzing the plasma mechanism of sub-THz emission from the heated loop footpoints in the chromosphere (Zaitsev, Stepanov, and Melnikov, 2013). The main contribution to the circuit resistance (Equation (7)) comes from the footpoints of a loop with relatively low conductivity caused by ion–atom collisions (the so-called Cowling conductivity). As for the loop eigen-frequency we have to consider

the whole loop, with a larger part in the corona. In the coronal part of the loop, the inequality $b^2 \gg 1$ is satisfied, and the frequency of the LRC-oscillations is

$$\omega_0 = \frac{c}{\sqrt{LC(I_0)}} \approx \frac{1}{(2\pi)^{1/2}\sqrt{\Lambda}} \frac{I_0}{cr_2^2\sqrt{n_2 m_\mathrm{i}}}. \tag{8}$$

Here, $\Lambda = \ln \frac{4l_2}{\pi r_2} - \frac{7}{4}$ and n_2 is the electron density in the coronal part of the loop, m_i is the ion mass. Equation (8) suggests that electric current oscillations are in-phase in all points of the loop as an equivalent electric circuit (lumped circuit approach). On the other hand, variations of the current propagate along the loop with the Alfvén velocity. Hence the in-phase condition requires the Alfvén time, $\tau_\mathrm{A} = l_2/c_{\mathrm{A}2}$, to be shorter than the oscillation period, $\tau_\mathrm{LRC} = 2\pi/\omega_0$. Since the Biot–Savart law gives $I_0 \approx cr_2 B_{\varphi 0}(r_2)/2$, the synchronism condition is (Zaitsev *et al.*, 2012)

$$\frac{B_{\varphi 0}(r_2)}{B_{z0}(0)} < 2\pi\sqrt{2\Lambda}\frac{r_2}{l_2}. \tag{9}$$

This means that the ratio of the azimuthal to the longitudinal components of the magnetic field of the loop should be low. This condition is consistent with the stability condition against the kink mode. Equation (8) describes Alfvén oscillations of the coronal loop with the wave vector $|\vec{k}| \approx r_2^{-1}$ directed almost perpendicular to the loop axis with the angle θ, such that $\cos\theta \approx (B_\varphi/B_z)$. In this case

$$\omega_\mathrm{A} = kc_\mathrm{A}\cos\theta \approx \frac{1}{r_2}\frac{\sqrt{B_z^2 + B_\varphi^2}}{\sqrt{4\pi n_2 m_\mathrm{i}}}\frac{B_\varphi}{B_z} \approx \frac{1}{\sqrt{\pi}}\frac{I_0}{cr_2^2\sqrt{n_2 m_\mathrm{i}}}. \tag{10}$$

Equation (10) coincides with Equation (8) with the coefficient Λ on the order of unity. Here, we take into account that $I_0 \approx B_\varphi cr_2/2$.

The quality of the oscillations

$$Q = \frac{1}{cR}\sqrt{L/C} \tag{11}$$

can be very high because of the high loop inductance and comparatively low circuit resistance (see below). From Equation (3) it follows that oscillations of a loop as an equivalent electric circuit are excited if the negative resistance exceeds the circuit resistance,

$$R(I_0) \le |V_\mathrm{r}|l_1/\left(r_1 c^2\right). \tag{12}$$

Zaitsev *et al.* (2001) have shown that the nonlinear character of the capacitance (Equation (5)) and the resistance (Equation (7)) on the amplitude of the current transforms Equation (3) into Equation (18) (see Appendix A). Solution of Equation (18) using the Van der Pol method yields the steady-state value of the oscillations' amplitude (Equation (26)): $y_\infty = 2\sqrt{\delta}$, where $\delta = \frac{|V_\mathrm{r}|l_1}{c^2 r_1 R(I_0)} - 1$. The steady-state amplitude is specified by the excess of the negative resistance of the photospheric emf over the active resistance of the equivalent electric circuit.

5. The Influence of RLC Oscillations on Sub-THz Emission from a Coronal Loop

We considered the influence of eigen-RLC-oscillations of a coronal loop on the modulation of sub-THz emission. Zaitsev, Stepanov, and Melnikov (2013) presented some arguments in

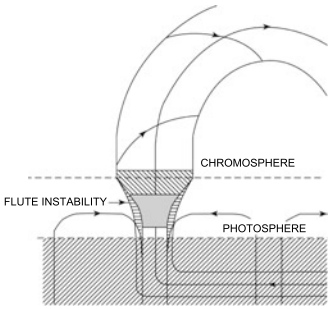

Figure 2 A sketch of a footpoint of a current-carrying loop. A sub-THz source (gray) and the free–free absorption domain above the source (dashed) are indicated. Plasma tongues penetrate into the loop because of the flute instability and induce the electric field.

support of the plasma radiation mechanism of the sub-THz emission from solar flares. They suggested that the source of sub-THz emission is located in the chromospheric footpoints of coronal loops. The main driver for electron acceleration and *in situ* heating of chromospheric plasma is the flute instability. The ballooning mode of flute instability leads to the penetration of the external chromospheric plasma into a current-carrying flare loop, which deforms the magnetic field at the loop footpoints (Figure 2). As a result, the electric current flowing along the loop changes and an inductive electric field emerges. The inductive electric field causes the acceleration of electrons to energies 500 – 2500 keV which do not escape from the chromosphere, providing the excitation of plasma waves and the heating of the chromospheric plasma.

From Appendix B it follows that the sufficient condition for the instability of the ballooning mode requires $n \geq n_{\rm a}$, which implies pre-heating of the chromospheric footpoints of a coronal magnetic loop to a temperature $T \geq 1.5 \times 10^4$ K. Such pre-heating can be provided by electric current dissipation due to Cowling resistivity related to ion–atom collisions. From Equation (40) it follows that the Joule heating rate exceeds radiation losses for the rate of photospheric convection, $V_{\rm r} \geq 4 \times 10^4$ cm s^{-1}. Horizontal velocities of convective flows in the vicinity of the boundaries of supergranulation cells, where the current-carrying magnetic loops are usually formed, are equal to $(3-5) \times 10^4$ cm s^{-1}. In 5 min photospheric oscillations, these velocities may reach $(1-2) \times 10^5$ cm s^{-1}. Therefore, it is expected that the region of manifestation of the flute-type instability effects in the chromosphere reaches the heights $h \geq 500$ km for densities of $n_{\rm tot} \leq 10^{15} - 10^{16}$ cm^{-3} (within the framework of the chromosphere model of Avrett and Loeser, 2008).

The scale of the height of the sub-THz source $\Delta z \approx 100-150$ km is on the order of that of the plasma "tongue" penetrating into the loop because of the flute instability. Accelerated electrons with the collisional mean free path, $\lambda < \Delta z$, do not escape from the source and contribute to the ionization in the chromosphere.

The origin of the modulation of sub-THz emission are the electric current oscillations in a coronal loop – an equivalent RLC-circuit. These current oscillations cause the modulation of the particle accelerator that modulates the plasma turbulence level and, as the result of Rayleigh and Raman scattering, modulates the sub-THz plasma emission. It is important to note that the sub-THz source must be quite compact, but the whole coronal loop oscillates with a frequency (Equation (8)) depending on the electric current value I_0 and on the parameters of the coronal part of the loop l_2, r_2, and n_2.

5.1. The Relation of the Flux-to-Repetition Rate

The Rayleigh and Raman scattering of plasma waves produces radio emission with fundamental and harmonic plasma frequencies, respectively. If the source optical depths with

respect to both conversion processes are lower than that with respect to the free–free absorption, the brightness temperatures of sub-THz emission are proportional to the level of plasma turbulence, w, at the fundamental frequency and to the squared of w at the harmonic (Zaitsev and Stepanov, 1983; Zaitsev, Stepanov, and Melnikov, 2013):

$$T_{b1} = \frac{a_1}{\mu_{c1}} \propto w \propto n_b \varepsilon_b, \qquad T_{b2} = \frac{a_2}{\mu_{c2}} \propto w^2 \propto (n_b \varepsilon_b)^2, \tag{13}$$

where $a_{1,2}$ and $\mu_{c1,2}$ are the emissivity and absorption coefficients at the fundamental and harmonic frequencies, respectively, n_b is the density of the electron beam, and ε_b is the electron beam energy.

Here we used the isotropic plasma approximation because the Langmuir frequency, $\nu_p \approx 200$ GHz corresponding to the electron density $n \approx 5 \times 10^{14}$ cm^{-3}, in the heated chromosphere is much higher than the electron gyrofrequency, $\nu_c = 8.4$ GHz ($\nu_p/\nu_c \approx 24 \gg 1$), even for a comparatively high magnetic-field value, $B = 3000$ G.

The electron beam energy, ε_b, is proportional to the value of accelerating electric field. In turn, the inductive electric field generated by the flute instability is proportional to the electric current (Zaitsev, Stepanov, and Melnikov, 2013). Thus, from Equation (13) it follows

$$T_{b1} \propto I(t), \qquad T_{b2} \propto I^2(t). \tag{14}$$

As the frequency of RLC-oscillations depends on the electric current, an important conclusion follows from Equations (8) and (14): in the framework of the plasma mechanism of sub-THz emission, the pulsation frequency grows with the emission intensity, and the time profile of the pulse-repetition rate, $\nu_r(t)$, should be similar to that of the flux. This conclusion is consistent with the observations (see Figure 1):

$$T_{b1} \propto \omega_0(t), \qquad T_{b2} \propto \omega_0^2(t). \tag{15}$$

If the emission at the fundamental tone prevails over that at the harmonic, the flux is proportional to the pulse-repetition rate (Figure 1a). If the emission at the harmonic dominates, the dependence of the emission flux on the modulation frequency follows a quadratic law. A possible illustration of this law is presented in Figure 1b. Note that two branches in Figure 1a, $F = k\nu_r(t)$ with k ($\nu = 405$ GHz) approximately equal to $4k$ ($\nu = 212$ GHz), can be explained by the well-known connection between the emission flux and the brightness temperature, $F \propto T_b \nu^2 S$, where S is the source area, which is approximately constant.

Consequently, in the framework of the plasma emission mechanism, the modulation of THz emission by eigen-oscillations of a coronal loop as a RLC circuit explains a very important characteristic of the observed rapid pulsations: the dependence of the emission flux on the repetition rate. Below we show that the electric-circuit approach also explains the other peculiarities of the pulsations under investigations.

5.2. Pulse Rate

From Equation (8) it follows that the pulsation repetition rate depends on the electric current and on the parameters of the coronal part of a flaring loop:

$$\nu_r = \frac{\omega_0}{2\pi} = \frac{1}{(2\pi)^{3/2}\sqrt{\Lambda}} \frac{I_0}{cr_2^2\sqrt{n_2 m_i}}. \tag{16}$$

Assuming a loop radius of $r_2 \approx 10^8$ cm and plasma density of $n_2 \approx 10^{10}$ cm^{-3}, from Equation (16) we obtain $\nu_r = (I_{11}/2)$ s^{-1}, where $I_{11} = 10^{-11} I(A)$. From Figure 3 of Kaufmann

et al. (2009) it follows that in the event of 4 November 2003, the pulse rate varied from 8.5 s^{-1} at the flare maximum to 0.2 s^{-1} after the burst. This corresponds to the decrease of the electric current from 1.7×10^{12} A to 4×10^{10} A. Note that a similar modification of the pulse period with the emission flux was observed at 17 GHz in the flare of 30 March 2001 (Zaitsev *et al.*, 2012). These electric-current estimates are reasonable for powerful flares. For example, vector-magnetograph measurements revealed almost the same current value at the footpoints of a flaring loop (Hagyard, 1988).

5.3. Q-Factor

For the events under study, the pulsation quality, Q, can be estimated independently assuming an effective electric-circuit resistance, $R_{\rm eff} \approx (W/I^2)$, where $W \approx 10^{18} - 3 \times 10^{20}$ W is the flare power, $I \approx 3 \times 10^{11}$ A is the current in a loop. As a result, we obtain $R_{\rm eff} \approx 10^{-5} - 3 \times 10^{-3}$ Ω. This estimated value of $R_{\rm eff}$ fits the highest value of the electric-circuit resistance well that is located near the region of the lowest temperature in the chromosphere at $h = 560$ km above the level of $\tau_{5000} = 1$, where $T = 4400$ K, $n_{\rm a} = 1.55 \times 10^{15}$ cm^{-3} and $n = 1.47 \times 10^{11}$ cm^{-3} (Avrett and Loeser, 2008). Indeed, using Equation (7) with $b \gg 1$, $I_0 = 3 \times 10^{11}$ A, $l_1 = 3 \times 10^7$ cm, $r_1 = 10^7$ cm, and $F_1 = 1$, taking into account Equation (37), we obtain the Cowling resistance, $R_{\rm eff} \approx 2 \times 10^{-3}$ Ω. Analogous calculations for $h = 175$ km, with $T = 5100$ K, $n_{\rm a} = 3.55 \times 10^{16}$ cm^{-3}, $n = 3.3 \times 10^{12}$ cm^{-3}, give $R_{\rm eff} \approx 3 \times 10^{-6}$ Ω.

The capacitance and inductance in the coil-condenser circuit are determined from Equations (5) and (4), respectively: $C \approx (r_2^2/l_2)(c^2/V_{{\rm A}\varphi}^2) = 3 \times 10^{10}$ cm $= 3 \times 10^{-2}$ F, $L \approx 10 l_2 \approx 10^{10}$ cm ≈ 10 H. In this way, we obtain the Q-factor, $Q \approx 6 \times 10^2 - 10^6 \gg 1$. Thus the LRC-model of a flaring loop yields a high pulsation quality, which corresponds to the observation of a long-duration pulse-train.

5.4. Pulse Amplitude

The amplitude of the pulses relative to the mean flux, $\Delta F/F$, is about 5 – 8 % at 212 and 405 GHz (Kaufmann *et al.*, 2009). Taking into account that $F \propto T_{\rm b}$, from Equation (14) it follows that in the framework of the plasma mechanism, the modulation depth is equal to the relative amplitude of electric-current oscillations in a circuit (in the case of the emission at the fundamental frequency), or equal to the double relative amplitude of current oscillations (in the case of emission at the harmonic). Equation (26) shows that in the steady-state regime of oscillations, the excess of negative resistance of the photospheric emf above the circuit resistance is low, $2\sqrt{\delta} = (5-8) \times 10^{-2}$, *e.g.* in a congruent circuit the nonlinear circuit resistance is consistent with the photospheric emf. Then from Equation (12) we obtain an independent estimate for the effective circuit resistance:

$$R_{\rm eff} \approx \frac{|V_{\rm r}| l_1}{r_1 c^2}. \tag{17}$$

Assuming the velocity of a plasma tongue under the conditions of ballooning instability on the order of the ion thermal velocity of the chromospheric plasma at the loop footpoints, and the tongue scale-height of about 100 – 500 km, we obtain $R_{\rm eff} \approx (1-5) \times 10^{-3}$ Ω. This does not contradict the estimate of $R_{\rm eff}$ made in Section 5.3.

Note that a deep modulation of the emission flux at 44 GHz (Kaufmann *et al.*, 2009) can be understood in terms of optically thin gyrosynchrotron emission. Using approximated formulas (Dulk, 1985), the modulation depth can be represented as $\Delta \approx$

$2(0.9\alpha - 0.22)\delta B/B$. Assuming that the power-law spectral index of accelerated electrons is $\alpha = 4.0$ for $\delta B/B = 0.1$, we obtain $\Delta \approx 0.7$.

5.5. Pulse Synchronism

The pulse synchronism at different frequencies can also be explained in the framework of the plasma emission mechanism. Indeed, if the condition described by Equation (9) is fulfilled, the model of a lumped circuit is realized and all parts of the loop oscillate in phase. Equation (9) shows that pulse synchronism is achieved in relatively short and "thick" loops and that it imposes restrictions on the shear of the loop's magnetic field. For instance, at $r_2 \approx 10^8$ cm, $l_2 \approx 10^9$ cm, and $B_z \approx 2 \times 10^3$ G, in-phase condition is true for an electric current $I_0 \leq 10^{12}$ A.

6. Discussion and Conclusions

Raulin *et al.* (2003) noted that the sub-THz emission fine structure consists of a mixture of spikes and pulsations. The fast pulse locations appear to be discrete and stationary in space ($5'' - 15''$), spread across the entire active region, and probably spaced by more than $30''$. As a possible origin of this fine structure, Raulin *et al.* (2003) proposed mechanisms of multiple explosive magnetic islands (Sturrock and Uchida, 1981), multiple-coalescence instabilities (Tajima, Brunel, and Sakai, 1982), or the interaction of multiple magnetic loops within the active region (Sturrock *et al.*, 1984). These models can indeed explain, to some extent, some properties of pulsations, but they encounter difficulties when attempting to explain the observed $F(\nu_r)$ dependence and the high Q-factor. On the other hand, the loop–loop coalescence in multi-loop flares that transport electric current (Khodachenko *et al.*, 2009) naturally explains the highly developed fine structure. This approach has something in common with the interpretation proposed by Sturrock *et al.* (1984); however, instead of the interaction of multiple magnetic fluxes, Khodachenko *et al.* (2009) suggested the presence of LRC-oscillations of current-carrying loops and loop–loop interactions.

Moreover, the model proposed here favors the hypotheses of discrete and successive energetic injections, quantized in energy. Indeed, small electric current variations produce variations of the azimuthal component of the magnetic field, B_ϕ, which, in turn, gives an electric field along the loop axis. This electric field is the reason for additional electron acceleration and injection into the emission region. As a result, a comparatively weak ($5 - 10$ %) emission pulse appears. In this way, a growing electric current gives enhanced emission at sub-THz and at the same time the pulse-repetition rate also grows. Because the flaring process is very unsteady, the loop plasma parameters can change radically. So the pulse period can also change and the observed pulsations are nonperiodical. Note that the plasma emission mechanism also explains two possible dependences of $F(\nu_r)$ in the considered events (Figure 1).

The pulsation model suggested here is based on the modulation of the sub-THz emission by eigen-oscillations of a coronal magnetic loop as an equivalent electric circuit and may explain the following peculiarities of the pulsations: i) the observed repetition rate, $\nu_r = 0.2 - 8$ s^{-1}, ii) the high Q-factor, $Q \geq 10^3$, iii) the small pulse amplitude, and iv) the pulse synchronism at different frequencies of the sub-THz emission. Moreover, the proposed model can explain the observed variations of the pulse-repetition rate with the variations of the sub-THz emission flux within the hypothesis of plasma emission. This is a strong additional argument in favor of the plasma emission mechanism of sub-THz radiation. Other models have difficulties attempting to explain all the characteristics of the observational data.

Acknowledgements The authors thank V. Makhmutov for discussions and an anonymous referee for valuable suggestions. This work was partially supported by RFBR grants No. 12-02-00616, 13-02-00044, 14-02-00133, and the Programs of the Russian Academy Presidium No. 22, 21. PK received partial support from the Brazil agencies FAPESP (grant no. 06/06847-1), CNPq and Mackpesquisa and US AFOSR.

Appendix A: Current Oscillation Amplitude

Taking into account the dependence of the nonlinear capacitance and resistance on the amplitude of the current in a magnetic loop, one can write the following expression instead of Equation (3) (Zaitsev *et al.*, 2001; Khodachenko *et al.*, 2009):

$$\frac{1}{c^2}L\frac{\mathrm{d}^2y}{\mathrm{d}t^2}+\left[R(I_0)(1+y)^2-\frac{|V_\mathrm{r}|l_1}{c^2r_1}\right]\frac{\mathrm{d}y}{\mathrm{d}t}+\frac{1}{C(I_0)}\left(1+\frac{3}{2}y+\frac{1}{2}y^2\right)y=0. \tag{18}$$

Introducing the dimensionless time $\tau=\omega_0 t$, Equation (18) can be written as

$$\frac{\mathrm{d}^2y}{\mathrm{d}\tau^2}-\varepsilon\left(\delta-2y-y^2\right)\frac{\mathrm{d}y}{\mathrm{d}\tau}+\left(1+\frac{3}{2}y+\frac{1}{2}y^2\right)y=0. \tag{19}$$

Here

$$\varepsilon=\frac{1}{Q},\qquad \delta=\frac{|V_\mathrm{r}|l_1}{c^2r_1R(I_0)}-1. \tag{20}$$

In the case of a high Q-factor, in Equation (19) $\varepsilon\ll 1$. Hence, the solution of (19) can be obtained by the Van der Pol method

$$y=A(\tau)\mathrm{e}^{\mathrm{i}\tau}+A^*(\tau)\mathrm{e}^{-\mathrm{i}\tau}, \tag{21}$$

where $A(\tau)$, $A^*(\tau)$ are time-dependent functions, which are slowly varying on the time scale equal to the oscillation period. Substituting (21) in (19) and averaging over the period, $T=2\pi$, we obtain the equation for $A(\tau)$:

$$\frac{\mathrm{d}A}{\mathrm{d}\tau}=\frac{1}{2}\left(\varepsilon\delta-\varepsilon|A|^2\right)A-\frac{3}{4}\mathrm{i}|A|^2A. \tag{22}$$

Assuming $A(\tau)=\frac{1}{2}a(\tau)\mathrm{e}^{\mathrm{i}\varphi(\tau)}$ and separating the real and imaginary parts in Equation (22), we obtain two equations for the amplitude and the phase:

$$\frac{\mathrm{d}a}{\mathrm{d}\tau}=\frac{1}{2}\varepsilon\left(\delta-\frac{1}{4}a^2\right)a, \tag{23}$$

$$\frac{\mathrm{d}\varphi}{\mathrm{d}\tau}=-\frac{3}{16}a^3. \tag{24}$$

As a result, we have the following solution for the oscillation amplitude:

$$a(\tau)=\frac{2\sqrt{\delta}}{[1+(\frac{4\delta-a_0^2}{a_0^2})\exp(-\varepsilon\delta\omega_0 t)]^{1/2}}. \tag{25}$$

We can see that the oscillation amplitude may vary from the initial value a_0 to the steady-state value $a_\infty = 2\sqrt{\delta}$. In the steady state, the solution is

$$y = \frac{I(t) - I_0}{I_0} = 2\sqrt{\delta}\cos\left[\omega_0\left(1 - \frac{3\sqrt{2}}{8}\delta^{3/2}\right)t\right]. \tag{26}$$

Thus, the nonlinearity of Equation (18) yields the steady-state value of the oscillations and a minor shift of the frequency from that in the linear case.

Appendix B: Flute-Type Instability in a Current-Carrying Magnetic Loop

Favorable conditions for the flute-type instability to develop exist in the vicinity of the chromospheric footpoints of magnetic loops. In this case, the sharp decrease of the plasma pressure with height results in the presence of magnetic-field curvature (effective gravitation), directed inside the loop. The curvature radius of the magnetic-field lines is on the order of the scale height of the inhomogeneous atmosphere (Priest, 1982),

$$R_c \approx \frac{k_B T}{m_i g}. \tag{27}$$

We use the relation (27) because near the chromospheric loop footpoints the loop's cross-section is proportional to the plasma's gas pressure and grows with the scale height (27). As a result, the loop becomes thicker and a magnetic-field curvature appears.

The magnetic-field curvature produces the centrifugal force

$$\vec{f}_c = \frac{2nk_B T}{R_c^2}\vec{R}_c, \tag{28}$$

which acts on a cubic centimeter of plasma with a density $\rho \approx (n + n_a)m_i$. Thus, the effective centrifugal acceleration of the chomospheric plasma around the footpoint of the loop is equal to

$$\vec{g}_c = (\vec{f}_c/\rho) = \frac{2k_B T}{m_i R_c^2}\frac{n}{n + n_a}\vec{R}_c, \tag{29}$$

where n and n_a are the number density of electrons and neutral atoms, respectively. Substituting (28) into (29), we obtain

$$g_c = 2g\frac{n}{n + n_a}. \tag{30}$$

The condition for the ballooning instability is

$$g_c - g\cos\theta > 0, \tag{31}$$

where θ is the angle between the direction of the curvature radius, R_c, and the vertical. If R_c is roughly perpendicular to g, the build-up time of the ballooning mode of the flute instability is

$$\tau_b = \frac{1}{2}\left(\frac{\lambda}{\pi g}\right)^{0.5}\left(\frac{n}{n + n_a}\right)^{-0.5}, \tag{32}$$

where λ is the perturbation wavelength. The estimate (32) corresponds to the most unstable case, when the perturbation wave-vector is perpendicular to the magnetic field (Priest, 1982). In the case of $n_a \ll n$

$$\tau_b \approx 2 \times 10^{-3} \lambda^{0.5} \text{ s}, \tag{33}$$

and perturbations with wavelengths $\lambda \approx 10^7$ cm (on the order of the loop radius in the chromosphere) develop in times on the order of 10 s.

It follows from (30) and (31) that the sufficient condition for the development of the instability is

$$n \geq n_a. \tag{34}$$

Under normal conditions in the chromosphere, the degree of ionization is small, $\sim 10^{-4}$, therefore, in order to increase it, a source of heating should exist. To determine the temperature to which the chromosphere should be heated so that the condition (34) is fulfilled, one can use the modified Saha formula, which is applicable under the lower-chromospheric conditions (Brown, 1973):

$$\frac{(n+n_a)x^2}{1-x} = 7.2 \times 10^{18} T^{0.5} \exp\left(-6.583 - \frac{1.185 \times 10^5}{T}\right), \tag{35}$$

where $x = n/(n+n_a)$. It follows from (35) that for the regions of the chromosphere with densities $n_{tot} = n + n_a = 10^{16}, 10^{15}, 10^{14}$ cm^{-3}, the instability criterion (34) is fulfilled when the corresponding layers are heated to temperatures of $T \approx 2 \times 10^4$ K, 1.5×10^4 K, 1.2×10^4 K, respectively. If a magnetic flux tube is formed by converging flows of photoshperic plasma with a velocity $V_r(r)$, then electric currents are generated within it, and their dissipation results in additional heating. The basic contribution to the dissipation is provided by the Cowling conductivity related to electron–atom collisions. Then the dissipation rate is determined by the formula (Sen and White, 1972; Zaitsev and Khodachenko, 1997)

$$q_J = \frac{n m_i \nu'_{ia} V_r^2 (1+x)}{(1-x)^2}. \tag{36}$$

Under chromospheric conditions, the basic contribution to the ion–atom collisions is made by the process of recharging, for which, within the temperature interval $4 \times 10^3 < T < 10^5$ K, we can write

$$\nu'_{ia} \approx 2.25 \times 10^{-11} n_a \sqrt{T}. \tag{37}$$

Hence

$$q_J = 3.76 \times 10^{-35} \frac{1+x}{1-x} (n+n_a) n \sqrt{T} V_r^2 \text{ erg cm}^{-3} \text{ s}^{-1}. \tag{38}$$

To increase the chromospheric temperature, the Joule heating rate should exceed the radiation losses. In the temperature interval $8 \times 10^3 < T < 2 \times 10^4$, the rate of radiation losses is determined by (Peres *et al.*, 1982)

$$q_r = \left(1.397 \times 10^{-8} T\right)^{6.15} (n+n_a) n. \tag{39}$$

From the condition $q_r \leq q_J$, we obtain the lower boundary for the rate of photospheric convection that provides pre-heating and the necessary ionization degree for the ballooning

mode of the flute instability to develop:

$$\begin{aligned} n + n_a &= 10^{14}\ \mathrm{cm}^{-3}, \qquad V_r \geq 2 \times 10^4\ \mathrm{cm\,s}^{-1}, \\ n + n_a &= 10^{15}\ \mathrm{cm}^{-3}, \qquad V_r \geq 4 \times 10^4\ \mathrm{cm\,s}^{-1}, \\ n + n_a &= 10^{16}\ \mathrm{cm}^{-3}, \qquad V_r \geq 4 \times 10^5\ \mathrm{cm\,s}^{-1}. \end{aligned} \tag{40}$$

References

Alfvén, H., Carlqvist, P.: 1967, *Solar Phys.* **1**, 220.
Avrett, E.H., Loeser, R.: 2008, *Astrophys. J. Suppl.* **175**, 229.
Brown, J.C.: 1973, *Solar Phys.* **29**, 421.
Cargill, P.J., Ghen, J., Garren, D.A.: 1994, *Astrophys. J.* **423**, 854.
Dulk, G.A.: 1985, *Annu. Rev. Astron. Astrophys.* **23**, 16.
Fleishman, G.D., Bastian, T.S., Gary, D.E.: 2008, *Astrophys. J.* **684**, 1433.
Fleishman, G.D., Kontar, E.P.: 2010, *Astrophys. J. Lett.* **709**, L127.
Hagyard, M.J.: 1988, *Solar Phys.* **115**, 107.
Huang, G., Qin, Z., Yao, Q.: 1996, *Astrophys. Space Sci.* **243**, 401.
Ionson, J.: 1982, *Astrophys. J.* **254**, 318.
Ji, H., Cao, W., Goode, P.R.: 2012, *Astrophys. J. Lett.* **750**, L25.
Kan, J.R., Akasofu, S.-I., Lee, L.C.: 1983, *Solar Phys.* **84**, 153.
Kaufmann, P., Strauss, F.M., Opher, R., Laporte, C.: 1980, *Astron. Astrophys.* **87**, 58.
Kaufmann, P., Raulin, J.-P., de Castro, C.G.G., Levato, H., Gary, D.E., Costa, J.E.R., *et al.*: 2004, *Astrophys. J. Lett.* **603**, L121.
Kaufmann, P., Levato, H., Cassiano, M.M., Correia, E., Costa, J.E.R., Giménez de Castro, C.G., *et al.*: 2008, In: Stepp, L.M., Gilmozzi, R. (eds.) *Ground-Based and Airborne Telescopes II*, *Proc. SPIE* **7012**, 70120-1.
Kaufmann, P., de Castro, C.G.G., Correa, E., Costa, J.E.R., Raulin, J.-P., Valio, A.S.: 2009, *Astrophys. J.* **697**, 420.
Khodachenko, M.L., Zaitsev, V.V., Kislyakov, A.G., Stepanov, A.V.: 2009, *Space Sci. Rev.* **143**, 112.
Kliem, B., Karlický, M., Benz, A.O.: 2000, *Astron. Astrophys.* **360**, 715.
Krucker, S., de Castro, G.C.G., Hudson, H.S., Trottet, G., Bastian, T.S., Hales, A.S., *et al.*: 2013, *Astron. Astrophys. Rev.* **21**.
Landau, L.D., Lifshitz, E.M.: 1984, *Electrodynamics of Continuous Media*, Pergamon Press, Elmsford.
Makhmutov, V.S., Raulin, J.-P., de Castro, C.G.G.: 2003, *Solar Phys.* **218**, 211.
Nakariakov, V.M., Hornsey, C., Melnikov, V.F.: 2012, *Astrophys. J.* **761**, 134.
Nakariakov, V.M., Melnikov, V.F., Reznukova, V.E.: 2003, *Astron. Astrophys. Lett.* **412**, L7.
Peres, G., Rosner, R., Serio, S., Vaiana, G.S.: 1982, *Astrophys. J.* **252**, 791.
Priest, E.: 1982, *Solar Magnetohydrodynamics*, Reidel, Dordrecht.
Qin, Z., Li, C., Fu, Q., Gao, Z.: 1996, *Solar Phys.* **163**, 383.
Raulin, J.-P., Kaufmann, P., de Castro, C.G.G., *et al.*: 2003, *Astrophys. J.* **592**, 580.
Sakai, J.I., Nagasugi, Y., Saito, S., Kaufmann, P.: 2006, *Astron. Astrophys.* **457**, 313.
Sen, N.K., White, M.L.: 1972, *Solar Phys.* **23**, 146.
Stepanov, A.V., Zaitsev, V.V., Nakariakov, V.M.: 2012, *Coronal Seismology: Waves and Oscillations in Stellar Coronae*, Wiley-VCH, New York, 221.
Stepanov, A.V., Zaitsev, V.V.: 2013, In: van Leeuwen, J. (ed.) *IAU Symp.* **291**, Cambridge Univ. Press, Cambridge, 505.
Stepanov, A.V., Kliem, B., Krüger, A., Hildebrandt, J., Garaimov, V.I.: 1999, *Astrophys. J.* **524**, 961.
Stepanov, A.V., Kliem, B., Zaitsev, V.V., Fürst, E., Jessner, A., Krüger, A., *et al.*: 2001, *Astron. Astrophys.* **374**, 1072.
Sturrock, P.A., Uchida, Y.: 1981, *Astrophys. J.* **246**, 331.
Sturrock, P.A., Kaufman, P., Moore, R.L., Smith, D.F.: 1984, *Solar Phys.* **94**, 341.
Tajima, T., Brunel, F., Sakai, J.: 1982, *Astrophys. J.* **258**, 45.
Tan, B., Yan, Y., Tan, C., Liu, Y.: 2007, *Astrophys. J.* **671**, 964.
Zaitsev, V.V.: 1971, *Solar Phys.* **20**, 95.
Zaitsev, V.V., Khodachenko, M.L.: 1997, *Radiophys. Quantum Electron.* **40**, 114.

Zaitsev, V.V., Stepanov, A.V.: 1983, *Solar Phys.* **88**, 297.
Zaitsev, V.V., Stepanov, A.V.: 1992, *Solar Phys.* **139**, 343.
Zaitsev, V.V., Stepanov, A.V., Melnikov, V.F.: 2013, *Astron. Lett.* **39**, 650.
Zaitsev, V.V., Stepanov, A.V., Urpo, S., Pohjolainen, S.: 1998, *Astron. Astrophys.* **337**, 887.
Zaitsev, V.V., Kislyakov, A.G., Urpo, S., Shkelev, E.I.: 2001, *Radiophys. Quantum Electron.* **44**, 765.
Zaitsev, V.V., Kislyakova, K.G., Altyntsev, A.T., Meshalkina, N.S.: 2012, In: Obridko, V.N., Georgieva, K., Nagovitsyn, Y.A. (eds.) *The Sun: New Challenges*, *Astrophys. Space Sci. Proc.* **30**, Springer, Berlin, 47.
Zheleznyakov, V.V.: 1997, *Emission of Astrophysical Plasma*, Yanus-K, Moscow (in Russian).